POLITECNICO DI TORINO
Repository ISTITUZIONALE

On the Trade-off Between Computational Complexity and Collaborative GNSS Hybridization

*Original*
On the Trade-off Between Computational Complexity and Collaborative GNSS Hybridization / Minetto, A., Falco, G., Dovis, F.. - ELETTRONICO. - (2019). (2019 IEEE 90th IEEE Conference on Vehicular Technology (VTC) Honolulu, Hawaii (USA) 22-25 September 2019) [10.1109/VTCFall.2019.8891571].

*Availability:*
This version is available at: 11583/2760486 since: 2019-10-15T09:26:43Z

*Publisher:*
IEEE

*Published*
DOI:10.1109/VTCFall.2019.8891571

*Terms of use:*

This article is made available under terms and conditions as specified in the corresponding bibliographic description in the repository

*Publisher copyright*
IEEE postprint/Author's Accepted Manuscript

©2019 IEEE. Personal use of this material is permitted. Permission from IEEE must be obtained for all other uses, in any current or future media, including reprinting/republishing this material for advertising or promotional purposes, creating new collecting works, for resale or lists, or reuse of any copyrighted component of this work in other works.

(Article begins on next page)

19 November 2026

# On the Trade-off Between Computational Complexity and Collaborative GNSS Hybridization

Alex Minetto
*Dept. of Electronics and Telecommunications, Politecnico di Torino*
Turin, Italy
alex.minetto@polito.it

Gianluca Falco
*Space and Navigation Technology LINKS foundation*
Turin, Italy
gianluca.falco@linksfoundation.com

Fabio Dovis
*Dept. of Electronics and Telecommunications, Politecnico di Torino*
Turin, Italy
fabio.dovis@polito.it

***Abstract*—In the last decades, several positioning and navigation algorithms have been developed to enhance vehicular localization capabilities. Thanks to ad-hoc communication networks, the exchange of navigation data and positioning solutions has been exploited to the purpose. This trend has recently suggested the extension of state-of-the art navigation algorithms to the hybridization of independent heterogeneous measurements within collaborative frameworks. In this paper an integration paradigm based on the combination of Global Navigation Satellite System (GNSS) observable measurements is analysed. In this work, a comparison among legacy Extended Kalman Filter (EKF) and a suboptimal Particle Filter (s-PF) is proposed. First we show that under the same assumptions in non-collaborative framework the s-PF easily overcome EKF performances at the cost of a higher computational cost. On the contrary, by analysing a realistic scenario in which a target agent is aided by a set of collaborating peers we showed that a hybridized EKF implementation allows reaching and overcome PF performance at the only expense of network connectivity among few GNSS receivers, while the proposed integration induces minor benefits for an efficient s-PF.**

***Index Terms*—GNSS, Extended Kalman Filter, Particle Filter, Navigation Performance, Collaborative Ranging**

## I. Introduction

In the last decades a considerable research effort has been spent in the field of vehicular navigation and positioning by addressing sensors integration to Global Navigation Satellite System (GNSS) [1]. In parallel, remarkable contributions to cooperative approaches have been proposed to enhance positioning and navigation performance in vehicular networks, mostly relying on end-to-end ad-hoc connectivity [2], [3]. The most effective implementations have addressed line-of-sight range information (e.g. UWB, Lidar, Sonar) and the integration of proprioceptive sensors as auxiliary source of information, while few contributions have focused on GNSS-based collaborative ranges obtained by means of non-Line-of-Sight network communication [4]. Next to the relevant opportunities offered by modern communication networks to vehicular navigation, the recent release of *raw measurements* in mass market devices has opened a number of opportunities for the development of improved positioning algorithms, by guaranteeing the access to measurements data prior to the positioning solution [5]. Similarly to previous solutions relying on cooperative estimation of positioning and navigation data, such as for example belief propagation [6], [7], we aim at reconsidering the exchange of raw GNSS data (i.e. satellite-to-user raw pseudorange measurements) to extract auxiliary range information that can be beneficial to improve both accuracy and precision of the navigation solution. The idea of overcoming the limits of LoS ranging through common satellites in visibility is appealing especially for the fully-connected devices contemplated within Intelligent Transportation Systems (ITS) and Smart Cities paradigms. The integration of auxiliary measurements is typically exploited by means of Kalman Filter (KF) which is an effective algorithm to perform a Bayesian estimation of the Position, Time and Velocity (PVT) of dynamic GNSS receivers. Despite KF is a good compromise in terms of accuracy and computational complexity, Particle Filter (PF) has become a popular alternative which can increase the estimation accuracy by means of Monte Carlo approach [8]. PFs have been extensively investigated in navigation for robotics and several solutions and optimizations have been discussed in literature [9]–[12] to fit a variety of different applications. Following previous contributions about collaborative inter-agent range estimation [13], [14] and the proposed integration in the positioning and navigation algorithms [15], [16], this work aims at comparing the accuracy of the two different Bayesian *navigation filters* (i.e. KF, PF) and at verifying the effectiveness of integrating a combination of asynchronous GNSS-based measurements for the improvement of the positioning accuracy.

The paper is organized as follows. Section II recalls the Hidden Markov Model (HMM), extended through the investigation of correlated inter-agent measurements. Section III provides a brief description of the implemented Bayesian navigation filters. Section IV illustrates the scenario used for the comparison and Section V gives a summary of the analysis. In Section VI, the findings of the work are summarized.

## II. Problem Statement

The estimation problem to be solved in positioning and navigation is often referred in literature to as *object tracking*, where the *object* can be indeed a GNSS receiver in the form of a stand-alone equipment or embedded in a number of possible devices (e.g. vehicular navigation systems, smartphones, smartwatches). As depicted in Figure 1, the problem

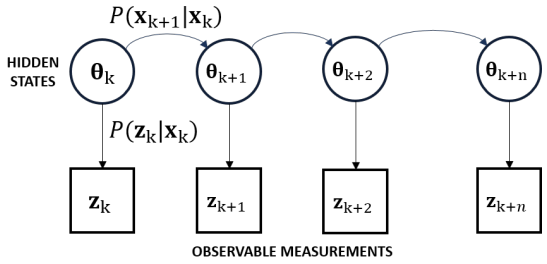



Fig. 1. Hidden Markov Model (HMM) for single agent state-space estimation.

is modelled as a Hidden Markov Model (HMM) where the *state space*, $\boldsymbol{\theta}_k$, of the target dynamic system can be known only through a set of *observable measurements*, $\mathbf{z}_k$ [8].

In the following, the state space vector is defined as

$$\boldsymbol{\theta}_k = \begin{bmatrix} x_k & y_k & z_k & b_k & \dot{x}_k & \dot{y}_k & \dot{z}_k & \dot{b}_k \end{bmatrix}. \tag{1}$$

Equation (1) describes the relevant information about the position, $\mathbf{x}_k = \begin{bmatrix} x_k & y_k & z_k \end{bmatrix}$, and the velocity $\dot{\mathbf{x}}_k = \begin{bmatrix} \dot{x}_k & \dot{y}_k & \dot{z}_k \end{bmatrix}$, of a generic GNSS receiver, provided in a conventional reference frame (i.e. Earth Centred Earth Fixed, East-North-Up). $b_k$ and $\dot{b}_k$ are respectively the bias and the drift of the local clock w.r.t. a reference time scale (GNSS time). Bayesian navigation filters are devoted to the joint estimation of the state vector and the associated error covariance matrix, $\mathbf{P}_{\theta,k} = \mathrm{E}\left[ \left( \boldsymbol{\theta}_k - \mathrm{E}\left( \boldsymbol{\theta}_k \right) \right) \left( \boldsymbol{\theta}_k - \mathrm{E}\left( \boldsymbol{\theta}_k \right) \right)^T \right]$, which describes the uncertainty on the estimated solution [17]. The state transitions, represented by the horizontal arrows in Figure 1, are associated to a *transition probability*, $p\left( \mathbf{x}_k | \mathbf{x}_{k-1} \right)$ which is defined accordingly to a *state transition function*

$$\boldsymbol{\theta}_{k+1} = f_k\left( \boldsymbol{\theta}_k, \mathbf{v}_k \right) \tag{2}$$

where $f_k$ is a generic function of the vector state, and $\mathbf{v}_k$ is a multivariate random variable describing the noise affecting the states. A sequence of noisy measurements is performed by the receiver at each discrete time instant $t_k$ and each measurement links the current state vector to a specific reference point (e.g. GNSS satellites, terrestrial anchors, etc.). The relationship between state and measurements is hence described by the prior probability $p\left( \mathbf{z}_k | \mathbf{x}_k \right)$, according to

$$\mathbf{z}_k = h_k\left( \boldsymbol{\theta}_k, \mathbf{w}_k \right) \tag{3}$$

where $h_k$ is a generic function linking the observation vector to $\boldsymbol{\theta}$ and $\mathbf{v}_k$ is a multivariate random variable describing the measurements noise. The analysis presented in this work will be focused on the quality of the position estimation, $\hat{\mathbf{x}}_k$, by comparing such a subset of (1) to the true experimental trajectory.

### *A. Combined observable measurements and exchange of position estimates*

As shown in Figure 2, auxiliary observable measurements are assumed to be generated by combining the measurements in $\mathbf{z}_k$. They can be used as a joint information about the estimation of the two states $\boldsymbol{\theta}_m$ and $\boldsymbol{\theta}_n$, or they can be exploited by one of the two agents as an auxiliary source of information, as assessed by means of the analysis of the Cramer Rao Lower Bound in a previous contribution [18].

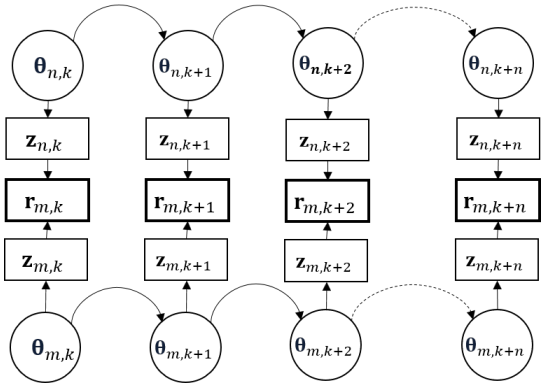



Fig. 2. Modified HMM for dual agent state-space estimation with collaborative and correlated measurement generation.

The computation of inter-agent measurements is based on a differential GNSS approach named Double Difference Ranging [13]. In order to combine the raw measurements related to common satellites in visibility, the users clocks must be aligned to a common reference time. All the cooperating agents are assumed to be roughly aligned to the GNSS time scale but providing asynchronous positioning solutions, thus inconsistent observables. According to the feasibility of a a coarse GNSS-time synchronization in vehicular networks [19], it has to be reminded that PVT solutions are provided independently among the receivers, therefore a doppler-based compensation stage has been implemented to mitigate the time-inconsistency of the measurements [20]. In standalone GNSS positioning, $\mathbf{z}$ consists of a *measurement vector* composed by $S$ satellite-to-receiver pseudorange measurements and $S$ pseudorange rates [21], retrieved by the received GNSS signal. When collaborative ranges are integrated in the measurement set, the measurement vector can be extended to incorporate also *inter-agent distances*, such that

$$\bar{\mathbf{z}}_\mathbf{k} = \begin{bmatrix} \mathbf{z}_k & \mathbf{r}_k \end{bmatrix}^T \tag{4}$$

where $\mathbf{r} = \begin{pmatrix} r_1 & r_2 & \dots & r_C \end{pmatrix}^T$, is a vector of collaborative ranges and $C$ is the number of collaborative agents and contributions. This point differentiates the approach from Real Time Kinematic (RTK) and Differential GNSS (a.k.a. DGPS) in which reference station with precisely known position are used to provide corrections or relative positioning data. The benefits introduced by the use of collaborating agents as anchors of opportunities or dynamic DGPS base stations has been assessed theoretically and experimentally, as in [18], [22].

## III. Navigation Filters

The two different Bayesian estimation approaches are briefly recalled in the following. Both EKF and suboptimal-PF (s-PF) will be used to compute an estimate of the full

state vector and of its covariance matrix by relying on the hybridized measurement vector (4).

### A. Hybrid Extended Kalman Filter (H-EKF)

The EKF is the most widespread algorithm for navigation in vehicular mobility. It is capable of an efficient and accurate position estimation and it allows a straightforward integration of auxiliary sensors [1].

The linearization required for the processing approximates (2) through

$$\boldsymbol{\theta}_{k+1} = \boldsymbol{\Phi}\left(\boldsymbol{\theta}_k, \mathbf{v}_k\right) \tag{5}$$

where $\boldsymbol{\Phi}$ is usually a time invariant matrix known as *state transition matrix*. Similarly, a linearization is applied to (3), thus considering

$$\bar{\mathbf{z}}_k = \bar{\mathbf{H}}_k\left(\boldsymbol{\theta}_k, \mathbf{w}_k\right) \tag{6}$$

where $\bar{\mathbf{H}}_k$ is named *Direct Cosine Matrix* (DCM) and describes the linearized relationship among all the measurements collected in $\bar{\mathbf{z}}_k$ and the state vector $\boldsymbol{\theta}_k$, at the discrete time $k$. Naming $\mathbf{H}_\rho$ the observation matrix related to the GNSS pseudorange measurements, the resulting *hybrid DCM* is defined as

$$\bar{\mathbf{H}}_k = \begin{bmatrix} \mathbf{H}_{\rho,k} & \mathbf{0}_{S\times 4} \\ \mathbf{0}_{S\times 4} & \mathbf{H}_{\rho,k} \\ \mathbf{H}_{r,k} & \mathbf{0}_{C\times 4} \end{bmatrix} \tag{7}$$

where the $s$-th row of the submatrix $\mathbf{H}_{\rho,k}$ can be expressed as

$$\left[\mathbf{H}_{\rho,k}\right]_s = \begin{bmatrix} (\mathbf{x}_s - \mathbf{x}_m)/||\mathbf{x}_s - \mathbf{x}_m|| & 1 \end{bmatrix} = \begin{bmatrix} \mathbf{h}_{s,m} & 1 \end{bmatrix} \tag{8}$$

where $\mathbf{x}_s$ and $\mathbf{x}_m$ are the satellite and user coordinates, respectively. $\mathbf{h}_{s,m}$ is the *unitary steering vector* pointing towards the $s$-th satellite and the unitary term is referred to the bias clock term common to all the measurements. Similarly, the set of equivalent steering vectors points at the collaborating agents so that the $r$-th row of $\mathbf{H}_{r,k}$ is defined as

$$\left[\mathbf{H}_{r,k}\right]_r = \begin{bmatrix} (\hat{\mathbf{x}}_c - \mathbf{x}_m)/||\hat{\mathbf{x}}_c - \mathbf{x}_m|| & 0 \end{bmatrix} = \begin{bmatrix} \mathbf{h}_{c,m} & 0 \end{bmatrix} \tag{9}$$

While the GNSS satellite position is known with a high accuracy from the ephemeris data, the *measurement equations* of the hybridized system (3) have to be referred to a rough estimate, $\hat{\mathbf{x}}_c$, of the agent position. This estimation must be provided along with raw measurements by collaborating agents. For the sake of brevity the implementation of the EKF for the estimation of the state vector is left to the exhaustive literature on the topic [23].

### B. Suboptimal implementation of a Particle Filter (s-PF)

The strategy of implementing a s-PF aims at providing a fair comparison among the filters. The proposed implementation does not exploit on purpose the capability of PF of dealing with non-Gaussian density function but it is worthy to consider that even restricting this condition, the accuracy of the estimation is higher than EKF. Furthermore, it is remarkable that an accurate modelling of the statistics of the measurements is not suitable in practice for an optimal implementation of the PF and the Gaussian approximation is hence applicable for a large variety of situations. The PF approximates the a posteriori distribution of (1)

$$p\left(\boldsymbol{\theta}_k|\mathbf{z}_k\right) \approx \sum_{i=1}^{N} w_k^{(i)} \delta\left(\boldsymbol{\theta}_k - \hat{\boldsymbol{\theta}}_k^{(i)}\right) \tag{10}$$

where $\delta$ is the Dirac delta function and $\hat{\boldsymbol{\theta}}_k^{(i)}$ is a propagated particle. The approximation is performed by generating and propagating a set of particles $\hat{\boldsymbol{\theta}}_k^{(i)}$ and associated weights $w_k^{(i)}$ according to the following steps:

1) *Initialization*: Generation of a set of $N$ particles $\hat{\boldsymbol{\theta}}_k^{(i)}$ according to $\hat{\boldsymbol{\theta}}_k \sim p(\hat{\boldsymbol{\theta}}_{k-1}, P_{\theta,k-1})$
2) *Prediction*: All the generated particles are propagated according to the dynamic system model (5)
3) *Weights computation*: The weights are obtained by relying on a pre-defined likelihood $p\left(\mathbf{z}_k|\hat{\boldsymbol{\theta}}_k^{(i)}\right)$ w.r.t. the expected measurements computed for each particle, the weights are hence defined as

$$w_k^{(i)} = \frac{\prod_n p\left(z_{n,k} - z_{n,k}^{(i)}\right)}{\sum_{i=1}^{N}\prod_n p\left(z_{n,k} - z_{n,k}^{(i)}\right)}. \tag{11}$$

4) *Resampling*: This step is of prominent importance since it guarantees the algorithm effectiveness avoiding particle collapse and overoptimistic covariance estimation. A number of resampling methods can be used to optimize the filter behaviour [24].
5) *Estimation*: The bayesian estimation is eventually given by the weighted average of the generated particles, as

$$\hat{\boldsymbol{\theta}}_k \approx \sum_{i=1}^{N} w_k^{(i)} \boldsymbol{\theta}_k^{(i)}. \tag{12}$$

In this study, the state transition in (5) was used for the prediction stage of the PF and a Gaussian likelihood was chosen for the weights computation (12), thus turning the current implementation in a suboptimal estimation algorithm. Differently from the integration proposed in [25], we take advantage on this sequential Bayesian method to improve the position estimation by merging such a different class of correlated range measurements.

### C. Computational Complexity

Let $n_\theta$ the dimension of the state vector, the computational complexity can be approximated to $\mathcal{O}(2n_\theta^3)$ and to $\mathcal{O}(Nn_\theta^2)$ for EKF and PF, respectively [10]. According to the number of elements of the state vector (1), it is worthy to consider that the execution time is comparable for the two navigation filters when $N \simeq 16$ [11]. These aspects is imperative for the implementation of the algorithms in low-power hardware architectures.

## IV. Test Scenario

The Bernoullian trajectory shown in Figure 3 was considered for the generation of the vehicular scenario. The trajectory was chosen among a set of geometrical paths centred at the point $C_1$. The four agents indicated by the black dots $C_c$ where

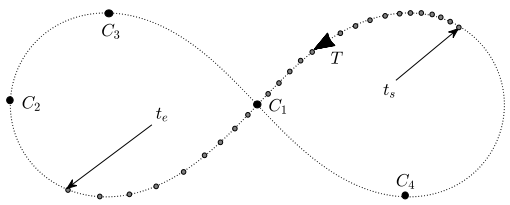



Fig. 3. Bernoullian Lemniscate test trajectory. The results are referred to the S-shaped portion starting from $t_s$ to $t_e$ and crossing the location of agent $C_1$.

$c \in (1, 4)$, are kept fixed while the target moves along the path according to a predefined uniformly accelerated dynamics, represented in Figure 3 by the small grey dots. The tangent speed of the target agent spans from $5$ m/s to $10$ m/s in a timespan of $60$ s. The true state vector (1) of each agent was generated with an update rate of $10$ Hz trough a Matlab® simulation environment. The true trajectories were stored as `.trj2` file to feed the IFEN NavX for the generation of GPS constellation and of the realistic satellite signals. Two different visibility conditions were considered in which the available satellite set has been randomly changed to observe the estimation performance of the two navigation filters in different conditions, as reported in Table IV. A set of 4 satellites were considered to satisfy the minimum conditions to initialize the positioning algorithm [21], while a set of 10 satellites simulates the open sky visibility of the GPS constellation. These alternatives also affected the quality of the inter-agent ranging and the overall estimation refinement obtained from the integration.

| **Visibility** | **No. of Satellites** | **Satellite IDs (PRN)** |
|---|---|---|
| Good (Open Sky) | 10 | 3,4,7,8,11,12,16,17,27,18 |
| Poor (Urban Canyon) | 4 | 4,7,8,27 |

## V. Results

A first set of results, shown in Figure 4, describes the improved average accuracy of the s-PF estimation w.r.t. to the EKF. The fact that the same accuracy is not affordable for an EKF, clearly remarks the benefits of using such a computational expensive algorithm for the PVT solution. In fact, while PF estimation can be asymptotically improved by increasing the number of particles, EKF already provides the best achievable solution which can be only improved by better environmental conditions experienced by the receiver. Although the considered implementation of the PF is suboptimal, an average accuracy improvement of $23.02\%$ for the 50th percentile of the error distribution has been achieved in

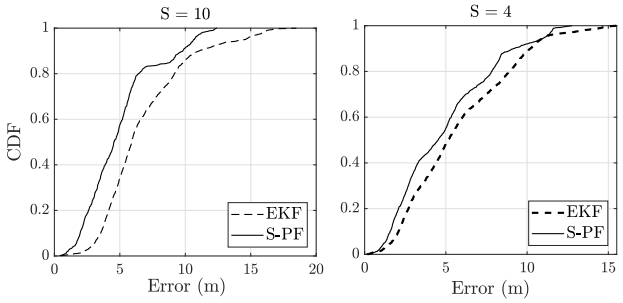



Fig. 4. CDFs of the estimated trajectory with plain s-PF ($N = 1000$) and EKF navigation filters.

good visibility. A reduced improvement of $12.36\%$ at the 50th percentile is instead observable in poor visibility conditions, as depicted in the right Cumulative Density Function (CDF) in Figure 4. According to the approximation of the computational complexity discussed in III, the usage of $1000$ particles requires a considerable computational effort, thus making the PF filter $62.5$ times slower in the estimation routine. By focusing

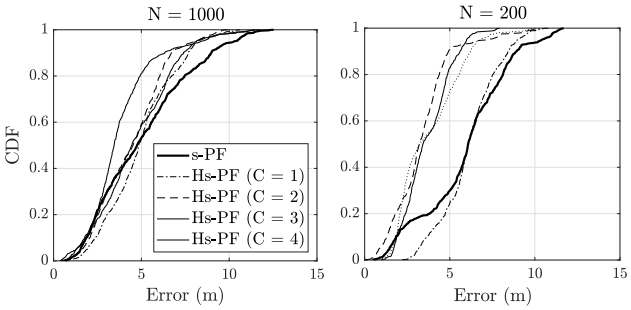



Fig. 5. CDFs of the estimated trajectory with Hybrid s-PF using different numbers of particles and varying the number of collaborative contributions.

on PF implementation, the results in Figure 5 show that a considerable advantage is provided by integrating auxiliary measurements when a lower number of particle is used for the PF-based estimation ($N = 200$). On the left plot, it can be noticed that the hybridization cannot provide a strong improvement, thus discouraging the cooperative effort when a high number of particle is used. On the other hand, the CDFs provided in Figures 6 and 7 confirm that the integration of collaborative range measurements can dramatically improve the EKF performance avoiding the increase of complexity required by the PF. The results show that EKF can be enhanced by integrating auxiliary correlated information more efficiently than what can be done by PF implementation. This suggests a trade-off in preferring collaborative solutions w.r.t. high-complexity navigation filters.

## VI. Conclusions

This paper compares the benefits of the integration of GNSS-only auxiliary measurements to positioning and navigation by proposing the inclusion of such observables in

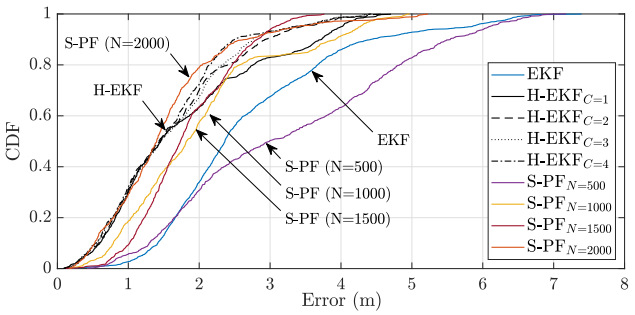



Fig. 6. CDF of EKF and PF trajectory estimation varying the number of particles and the number of collaborative contributions in good satellite visibility.

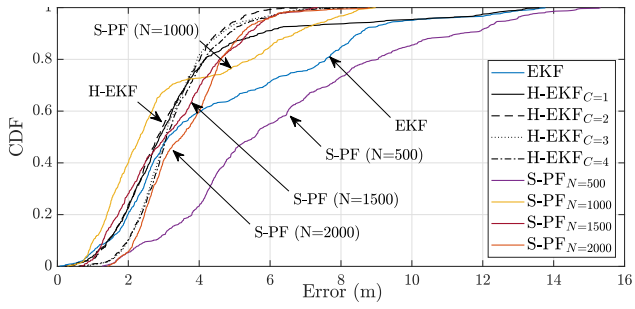



Fig. 7. CDF of EKF and PF trajectory estimation varying the number of particles and the number of collaborative contributions in poor satellite visibility.

the HHM model. The analysis were performed along a low-dynamics portion of a Bernoullian trajectory to properly compare the performance of an EKF and a suboptimal PF in different satellites visibility conditions. The s-PF reaches better accuracy and precision performance at a high computational cost while EKF offers practicable computational complexity although it leads to lower accuracy. The accuracy improvement provided by multi-agents collaborative range measurements is less significant when a high number of particles is used for PF position estimation. On the other hand, the EKF-based integration considerably increase the accuracy of the estimation reaching values close to highly-complex s-PF and by also maintaining a lower computational complexity. Further investigations are expected to explore the integration of sensors and cooperative strategies with specific optimizations for both the navigation filters.

## References


[1] M. S. Grewal, L. R. Weill, and A. P. Andrews, *Global positioning systems, inertial navigation, and integration*. John Wiley & Sons, 2007.

[2] M. A. Hossain, I. Elshafiey, and A. Al-Sanie, "Cooperative vehicular positioning with vanet in urban environments," in *2016 IEEE Asia-Pacific Conference on Applied Electromagnetics (APACE)*, Dec 2016, pp. 393–396.

[3] F. Shen, J. W. Cheong, and A. G. Dempster, "A DSRC doppler/IMU/GNSS tightly-coupled cooperative positioning method for relative positioning in VANETs," *The Journal of Navigation*, vol. 70, no. 1, pp. 120–136, 2017.

[4] N. Alam, A. T. Balaei, and A. G. Dempster, "Positioning enhancement with double differencing and DSRC," in *ION GNSS*. Citeseer, 2010, pp. 20–24.

[5] N. Gogoi, A. Minetto, N. Linty, and F. Dovis, "A controlled-environment quality assessment of android gnss raw measurements," *Electronics*, vol. 8, no. 1, 2018. [Online]. Available: https://www.mdpi.com/2079-9292/8/1/5

[6] M. A. Caceres, F. Penna, H. Wymeersch, and R. Garello, "Hybrid GNSS-terrestrial cooperative positioning via distributed belief propagation," in *2010 IEEE Global Telecommunications Conference GLOBECOM 2010*, Dec 2010, pp. 1–5.

[7] H. Kim, S. W. Choi, and S. Kim, "Connectivity information-aided belief propagation for cooperative localization," *IEEE Wireless Communications Letters*, vol. 7, no. 6, pp. 1010–1013, Dec 2018.

[8] N. Gordon, B. Ristic, and S. Arulampalam, "Beyond the kalman filter: Particle filters for tracking applications," *Artech House, London*, vol. 830, p. 5, 2004.

[9] M. S. Arulampalam, S. Maskell, N. Gordon, and T. Clapp, "A tutorial on particle filters for online nonlinear/non-gaussian bayesian tracking," *IEEE Transactions on Signal Processing*, vol. 50, no. 2, pp. 174–188, Feb 2002.

[10] F. Gustafsson, "Particle filter theory and practice with positioning applications," *IEEE Aerospace and Electronic Systems Magazine*, vol. 25, no. 7, pp. 53–82, July 2010.

[11] F. Gustafsson, F. Gunnarsson, N. Bergman, U. Forssell, J. Jansson, R. Karlsson, and P. . Nordlund, "Particle filters for positioning, navigation, and tracking," *IEEE Transactions on Signal Processing*, vol. 50, no. 2, pp. 425–437, Feb 2002.

[12] F. Daum, "Nonlinear filters: beyond the kalman filter," *IEEE Aerospace and Electronic Systems Magazine*, vol. 20, no. 8, pp. 57–69, Aug 2005.

[13] M. Tahir, S. S. Afzal, M. S. Chughtai, and K. Ali, "On the accuracy of inter-vehicular range measurements using GNSS observables in a co-operative framework," *IEEE Transactions on Intelligent Transportation Systems*, pp. 1–10, 2018.

[14] D. Yang, F. Zhao, K. Liu, H. B. Lim, E. Frazzoli, and D. Rus, "A GPS pseudorange based cooperative vehicular distance measurement technique," in *2012 IEEE 75th Vehicular Technology Conference (VTC Spring)*, May 2012, pp. 1–5.

[15] A. Minetto, A. Nardin, and F. Dovis, "Tight integration of gnss measurements and gnss-based collaborative virtual ranging," in *31st International Technical Meeting of the Satellite Division of The Institute of Navigation (ION GNSS+ 2018)*, September 2018, pp. 2399–2413.

[16] K. Liu, H. B. Lim, E. Frazzoli, H. Ji, and V. C. S. Lee, "Improving positioning accuracy using GPS pseudorange measurements for cooperative vehicular localization," *IEEE Transactions on Vehicular Technology*, vol. 63, no. 6, pp. 2544–2556, July 2014.

[17] S. M. Kay, *Fundamentals of statistical signal processing, volume I: Estimation theory (v. 1)*, 1993.

[18] A. Minetto, "A theoretical study on the benefits of integrating gnss and collaborative relative ranges," in *Proceedings of the 32th International Technical Meeting of The Satellite Division of the Institute of Navigation (ION GNSS+ 2019)*, Sep 2019.

[19] K. F. Hasan, Y. Feng, and Y. Tian, "Gnss time synchronization in vehicular ad-hoc networks: Benefits and feasibility," *IEEE Transactions on Intelligent Transportation Systems*, vol. 19, no. 12, pp. 3915–3924, Dec 2018.

[20] F. de Ponte Müller, A. Steingass, and T. Strang, "Zero-baseline measurements for relative positioning in vehicular environments," in *Sixth European Workshop on GNSS Signals and Signal Processing*, 2013.

[21] E. D. Kaplan and C. Hegarty, *Understanding GPS/GNSS: principles and applications*. Artech House, 2017.

[22] M. Rohani, D. Gingras, and D. Gruyer, "A novel approach for improved vehicular positioning using cooperative map matching and dynamic base station dgps concept," *IEEE Transactions on Intelligent Transportation Systems*, vol. 17, no. 1, pp. 230–239, 2015.

[23] R. G. Brown and P. Y. C. Hwang, *Introduction to random signals and applied Kalman filtering: with MATLAB exercises*. John Wiley & Sons, Inc., 2012.

[24] T. Li, M. Bolic, and P. M. Djuric, "Resampling methods for particle filtering: classification, implementation, and strategies," *IEEE Signal Processing Magazine*, vol. 32, no. 3, pp. 70–86, 2015.

[25] F. Sottile, H. Wymeersch, M. A. Caceres, and M. A. Spirito, "Hybrid GNSS-terrestrial cooperative positioning based on particle filter," in *2011 IEEE Global Telecommunications Conference - GLOBECOM 2011*, Dec 2011, pp. 1–5.